THE ROLE OF MICROCRACKS IN THERMALLY SPRAYED MATERIALS

F. KROUPA

Institute of Plasma Physics of ASCR
18221 Prague, Czech Republic

ABSTRACT

Mechanical properties of thermally sprayed materials, especially of ceramics, are strongly influenced by the high density of mesoscopic defects, microcracks of dimensions between a few μm up to tens of μm. The linear elastic stress-strain relations are valid at very small stresses only, with small Young's moduli due to elastic openings of microcracks. The increase of Young's moduli under compressive stresses , caused by elastic closures of microcracks and leading to nonlinear elastic behaviour, is analysed theoretically. Fracture and delamination of sprayed coatings, which proceeds by interconnection of microcracks at high stresses, is discussed.

KEYWORDS

Thermal spray, ceramic coatings, microcracks closure, stress-strain relations.

INTRODUCTION

Thermal spraying is a process in which the material in the powder form (with grading between 20 and 150μm) is melted, accelerated to a high velocity (20m/s up to 1000m/s) and deposited on the substrate. Different techniques of thermal spraying are used, e.g., plasma spraying, detonation-gun spraying, high velocity oxy-fuel spraying etc. To improve the adhesion of the coating to the substrate, the surface of the substrate should first be adequately prepared by surface roughening, usually by grit-blasting [1].

The microstructure of sprayed materials is complex. It consists of irregular thin lamellae known as "splats", formed by rapid solidification of the impacted molten droplets, of diameters between 100 and 300μm and heights between 2 and 10μm. For the spraying direction x_3 , the splats are approximately parallel to the spraying plane x_1x_2 (Fig.1). The splats are polycrystalline and consist usually of irregular fine columnar grains, elongated approximately in the x_3 direction. Thermal spraying may be accompanied by a change in the chemical composition, by a selective evaporation of a component of the powder or by interaction with the spraying atmosphere, e.g., by oxidation. Rapid cooling may result in formation of unusual or unstable crystal phases, in special cases even in an amorphous structure. Usually, imperfect bonds between the splats and substrate and between the individual splats develop during the rapid cooling.

The total porosity of the sprayed materials is usually between 2 and 15% and is mostly due to four families of defects (Fig.1):

(i) large irregular pores between the splats,
(ii) small spherical pores inside the splats,

(iii) imperfect bonding between the splats along the interfaces approximately parallel to the spraying plane x_1x_2 ; the unbonded regions will be referred to as the intersplat cracks,

(iv) microcracks approximately perpendicular to the spraying plane x_1x_2 formed inside the splats during their rapid cooling after solidification. They form an irregular microcrack pattern with microcrack normals distributed in the x_1x_2 planes, and will be referred to as the intrasplat cracks.

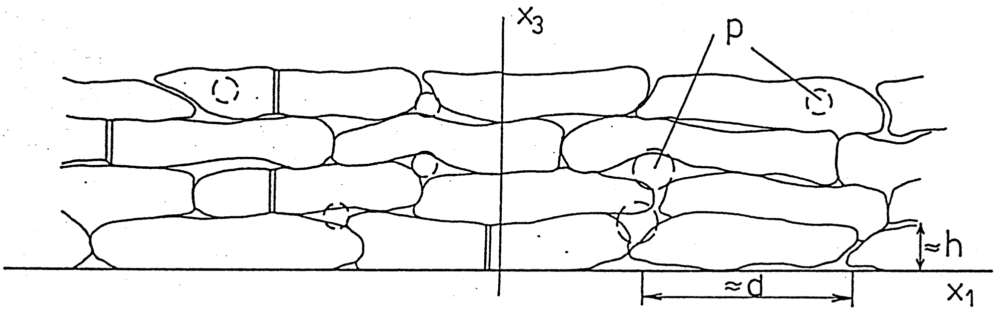

Fig.1. Schematic microstructure of sprayed materials: splats with imperfect bonds—intersplat cracks parallel to the spraying plane x_1x_2 , intrasplat cracks perpendicular to the x_1x_2 plane, approximately spherical pores between and inside the splats.

Although the intersplat and intrasplat cracks represent only a small part of the total porosity, they are believed to be the main factor causing the decrease of Young's moduli (due to elastic openings of the microcracks) and the elastic anisotropy. The intersplat cracks lead to the decrease of Young's modulus E_3 in the spraying direction x_3, while the intrasplat cracks lead to the decrease of Young's moduli E_1 in the directions lying in the x_1x_2 plane. This effect is more pronounced in ceramic than in metallic materials [1].

High macroscopic residual stresses usually appear in thermally sprayed coatings [2]. They can be divided into three groups from the point of view of their origin:

a. Quenching (or primary) residual stresses develop during the deposition process through a fast thermal contraction of solidified splats: they cool from the melting point down to the relatively low deposition temperature, i.e., the temperature of the substrate and of the previously deposited splats. The quenching stresses are tensile in the new deposited splats and are practically independent of the substrate properties.
b. Differential thermal contraction (or secondary) residual stresses appear when the substrate with the completed coating is cooled from the deposition temperature (usually a few hundred ^{o}C) to the ambient temperature. The secondary stresses depend on the difference of coefficients of thermal expansion of the coating and substrate and can be tensile or compressive.
c. In metal coatings deposited with a high velocity of the impacted droplets (e.g., by detonation spraying) also peening compressive stresses are produced.

The resulting residual stresses are sensitive to the parameters of the spraying technology used and may be a function of the distance x_3 from the interface, especially in thick coatings. There is a close connection between the quenching stresses and intrasplat cracks. The thermal contraction of the splats due to cooling from the melting temperature to the deposition temperature is of the order of 1% and the corresponding quenching stresses would be high, of the order of 10 GPa. However, these stresses relax for the main part during cooling, in metals by plastic deformation and microcracking, in ceramics preferentially by microcracking. Therefore, intrasplat cracks are formed as a process of relaxation of the quenching stresses. The resulting quenching stresses are usually smaller in ceramics than in metals.

A typical thickness of thermally sprayed coatings is between 0.2mm and 1mm. However, also free-standing parts are manufactured by thermal spraying, usually by air plasma spraying of ceramics. They are prepared as thick coatings (of thickness up to 10mm) and the substrate is then removed, e.g., by dissolution or by separation along the interface [3]. The distribution of microcracks in the free-standing parts remains the same as in the coatings, however, the residual stresses partly relax and partly redistribute during separation. Plasma spraying can be considered as a special technology of production of ceramic parts [4].

Microcracks of high density influence considerably various properties of sprayed materials, some of them in a negative way, but some in a positive way. The delamination of coatings under external loading, by thermal stresses and also by residual stresses proceeds by interconnection of microcracks in the interface. Fracture proceeds by interconnection of intrasplat cracks. On the other hand, elastic openings of the intrasplat cracks (leading to smaller Young's moduli) allow the ceramic coating to follow the deformation of the substrate to deformations 0.1 up to 0.2% without formation of macroscopic cracks. The microcracks also seem to improve the thermal-shock resistance of sprayed materials. The intersplat cracks decrease the thermal conductivity of sprayed coatings (for ZrO_2 coatings from the bulk value λ=2Wm^{-1}K^{-1} to the value $\lambda \cong 0.5$Wm^{-1}K^{-1}) and improve their function as thermal barriers [1].

In this paper, four specific problems of mechanical properties of sprayed materials will be discussed and the differences between the ceramic and metallic materials pointed out:

1.The decrease of Young's moduli due to elastic openings and partial closings of microcracks will be analysed, using a simplified model.

2.The nonlinear effect caused by elastic closing of microcracks by compressive stresses will be discussed.

3.The effect of tensile stresses and the behaviour of the surface region of sprayed materials will be mentioned.

4.Some comments will be given on the complex problems of the coating delamination and fracture, more from the point of view of the physical processes than the fracture mechanics.

EFFECT OF MICROCRACKS ON ELASTIC PROPERTIES

Experiments show that coatings and free-standing parts manufactured by thermal spraying have much lower elastic stiffness constants, twice up to three times less for metals and three times up to ten times for ceramics, than the corresponding bulk materials. Moreover, they have different Young's moduli E_1 and E_3 in the directions parallel and perpendicular to the spraying plane [1].

A series of theoretical papers [5-9] on explanation of the low values of elastic moduli has already been published. A special model of explanation of small Young's modulus E_3 in the x_3 direction is proposed in [5]. The splats are assumed to be bonded only along small areas of interfaces parallel to the x_1x_2 plane and the soft elastic response is explained as the result of bending of the unbonded parts of the splats.

The basic idea in papers [6-9] is common. The material is considered as a linear elastic isotropic continuum characterised by two elastic constants, Young's modulus E_0 and Poisson's ratio ν_0 , corresponding to a well sintered material. The microcracks are modelled as flat hollow rotational ellipsoids, randomly distributed in the continuum as two families: intersplat cracks parallel to the x_1x_2 plane and intrasplat cracks with normals randomly distributed in the x_1x_2 planes. Also a small effect of approximately spherical pores is taken into account by a random distribution of spherical cavities. The body is then anisotropic with the so-called transverse isotropy [10], characterised by five independent elastic constants. The dependence of these elastic constants on crack densities and on porosity is derived in papers

[6-9] with increasing accuracy and the effect of microcracks is in principle well explained. The cracks are assumed to be sufficiently opened so that the same elastic behaviour in tension and in compression follows.

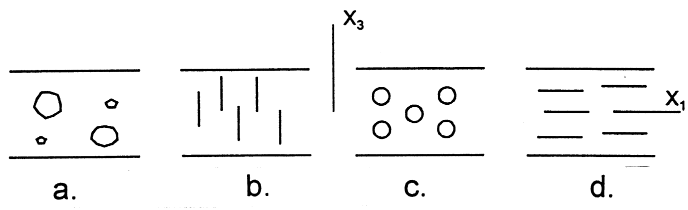

Fig.2. Theoretical model of the defect structure: a. irregular and spherical pores, b. cracks with normals in the x_1 direction, c. cracks with normals in the x_2 direction, d. cracks with normals in the x_3 direction.

We shall modify the results of paper [7] for another distribution of intrasplat cracks which will be suitable for discussion of the effect of compressive stresses in the next section. Besides the pores and intersplat cracks parallel to the x_1x_2 plane, two families of intrasplat cracks will be considered, the first with normals in the x_1 direction (chosen in the direction of the relative motion of the spraying gun and the sprayed body) and the second in the x_2 direction. For such distribution of type 1, 2 and 3 cracks (Fig.2), the axes x_1, x_2 and x_3 are preferential directions in the sprayed material and the principal axes of orthotropic symmetry, characterised by nine elastic constants. The linear Hooke's law between small deformations de_{ij} and small stresses $d\sigma_{ij}$ can then be written in the form [10]

$$
\begin{aligned}
de_{11} &= (1/E_1)\, d\sigma_{11} - (\nu_{12}/E_1)\, d\sigma_{22} - (\nu_{13}/E_1)\, d\sigma_{33}\,, \\
de_{22} &= -(\nu_{21}/E_2)\, d\sigma_{11} + (1/E_2)\, d\sigma_{22} - (\nu_{23}/E_2)\, d\sigma_{33}\,, \\
de_{33} &= -(\nu_{31}/E_3)\, d\sigma_{11} - (\nu_{32}/E_3)\, d\sigma_{22} + (1/E_3)\, d\sigma_{33}\,, \\
de_{23} &= [1/(2G_{23})]\, d\sigma_{23}, \quad de_{13} = [1/(2G_{13})]\, d\sigma_{13}, \quad de_{12} = [1/(2G_{12})]\, d\sigma_{12}
\end{aligned}
\tag{1}
$$

where, because of the symmetry of elastic compliances,

$$\nu_{12}/E_1 = \nu_{21}/E_2\,, \quad \nu_{13}/E_1 = \nu_{31}/E_3\,, \quad \nu_{23}/E_2 = \nu_{32}/E_3\,. \tag{2}$$

The defect structure of the sprayed materials will be modelled by spherical pores of radii R_k and by circular cracks of radii r_{1k} , r_{2k} and r_{3k} . The porosity p, $0<p<<1$, is mainly due to irregular, approximately spherical pores between the splats, and to smaller extent also to spherical pores inside the splats. The effect of cracks on the elastic constants can be characterised by the so-called scalar crack densities ρ per unit volume [6-9, 11, 12], in our case by ρ_1 , ρ_2 and ρ_3 . They can be expressed as

$$
\begin{aligned}
&p = (1/V)\sum_{k=1}^{n}(4/3)\pi R_k^3, \\
&\rho_1 = (1/V)\sum_{k=1}^{m} r_{1k}^3, \rho_2 = (1/V)\sum_{k=1}^{p} r_{2k}^3, \rho_3 = (1/V)\sum_{k=1}^{q} r_{3k}^3.
\end{aligned}
\tag{3}
$$

The effect of cracks is not given by their areas (proportional to r^2) but by the “adjoined volumes”: a larger crack has a larger effect than smaller cracks of the same total area have. The dependence of the nine elastic constants in eq. (1) and (2) on p, ρ_1, ρ_2 and ρ_3 can be constructed using the results in [11,12] as a sum of the effects of porosity and the three sets of parallel cracks with normals in the x_1 , x_2 and x_3 directions, as

$$1/E_i = (1/E_0) \{ 1 + [p/(1-p)] c_0 + [1/(1-p)] a_0 \rho_i \}, \quad i=1, 2, 3,$$

$$\nu_{ij}/E_i = (1/E_0) \{ \nu_0 + [p/(1-p)] c_1 \} , \quad i \neq j , \tag{4}$$

$$1/G_{ij} = [2(1+\nu_0)/E_0] \{ 1 +[p/(1-p)] c_2+[1/(1-p)] a_1 (\rho_i +\rho_j) \} , \quad i \neq j$$

where the positive constants c_0 , c_1 , c_2 , a_0 and a_1 depend on Poisson’s ratio ν_0 ,

$$c_0 = 3(1-\nu_0)(9+5\nu_0)/[2(7-5\nu_0)], \quad c_1 = 3(1-\nu_0)(1+5\nu_0)/[2(7-5\nu_0)], \; c_2 = 15(1-\nu_0)/[2(7-5\nu_0)],$$

$$a_0 = 16(1-\nu_0^2)/3, \quad a_1 = 16(1-\nu_0)/[3(2-\nu_0)]. \tag{5}$$

Note that compliances ν_{ij}/E_i characterising the lateral deformations do not depend on the crack densities ρ_i and are influenced only by porosity p. No summation convention over the repeated indexes is used in this paper.
The interaction between pores and cracks is taken into account in eq.(4) in a simplified way in the scheme of the effective stress field, and is expressed by terms 1/(1-p) [11,12].
For fixed porosity p and crack densities ρ_i , the elastic compliances in eq.(4) can be taken as the elastic constants of sprayed materials in Hooke’s law (1), as a first order approximation for small deformations e_{ij} and small stresses σ_{ij} written instead of de_{ij} and $d\sigma_{ij}$, respectively.
As an example, the dependence of E_1/E_0 on the scalar crack density ρ_1 is shown in Fig.3 for two values of porosity p and three values of Poisson’s ratio ν_0 .

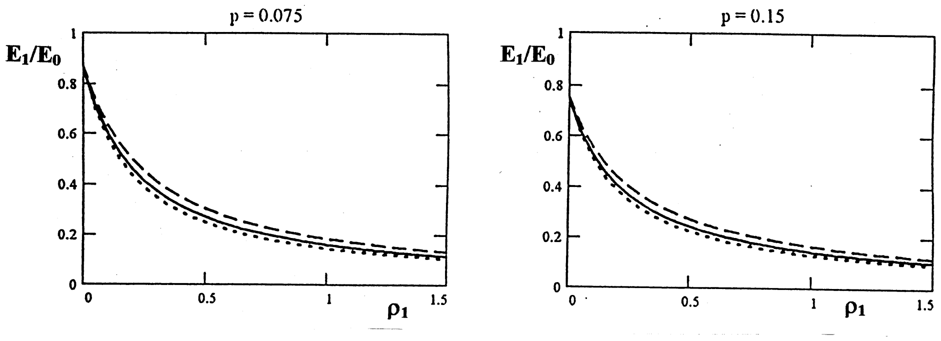

Fig.3. Dependence $E_1(\rho_1)/E_0$ for porosities p=0.075 and p=0.15. Full curves: ν_0=1/3; dotted curves: ν_0=0; dashed curves: ν_0=1/2.

NONLINEAR BEHAVIOUR DUE TO COMPRESSIVE STRESSES

Stress-strain relations

The effect of hydrostatic pressure on the velocity of elastic waves, which depends on elastic constants, is an important phenomenon in geophysics. In the theoretical papers [13,14] this effect is explained by the closing of microcracks present in the rocks, although usually to a smaller extent than in plasma-sprayed ceramics. Under hydrostatic pressure the bulk modulus of rocks increases, and the effect is found to be purely elastic and reversible [13]. On the other hand, under uniaxial compression Young's modulus also increases with compressive stress, however, the effect is not purely elastic and inelastic hysteresis appears during stress cycling [14]. This is explained by the relative shear displacements along the surfaces of cracks forming different angles with the stress axis, which leads to friction and energy absorption. These effects have been experimentally confirmed [13-17] and are well recognised in geophysics.

Similar, but more pronounced effects of compressive external or residual stresses on elastic moduli can be expected in thermally sprayed materials, especially in plasma sprayed ceramics with high density of microcracks, as discussed first in [18].

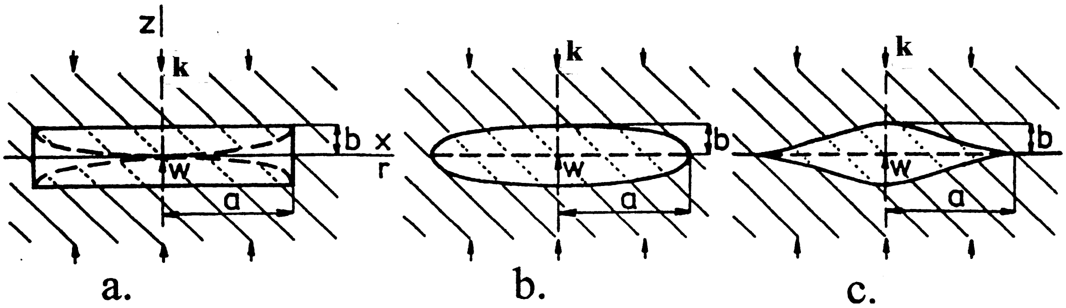

Fig.4.Crack closure.

Uniaxial pressure k acting in the direction z perpendicular to the crack plane (Fig.4) tends to close the crack. One crack in an infinite isotropic continuum characterised by elastic constants E_0 and ν_0 will be considered for simplicity. For an open circular crack, penny-shaped (Fig.4a) or oblate rotational ellipsoid (Fig.4b) with half axes a and b, b<<a, the elastic displacement w in the z direction in dependence on radial co-ordinate r is elliptical. It reaches at the crack centre, r=0, the value $w=(4/\pi)(1-\nu_0^2)(k/E_0)a$. The crack will close when w=b at closing pressure k_c, given by

$$k_c/E_0 = K\,(b/a) \qquad (6)$$

where the constant $K=\pi/[4(1-\nu^2)]$. The closing pressure is proportional to the crack aspect ratio b/a . At this pressure, the penny-shaped crack starts to close in the middle while the ellipsoidal crack closes completely. The sharp crack depicted in Fig. 4c closes continuously with increasing k. The closing pressure is not sensitive to the crack form. For example, for an elliptic crack in two-dimensional elasticity, the constant K in eq.(6) under plane strain conditions (crack infinite in the y direction) equals $K=1/[2(1-\nu^2)]$ and under plane stress conditions (crack in a plate thin in the y direction) K=1/2.

The effect of external stresses σ_{ij} on crack densities ρ_i will now be taken into account, whereas small changes of porosity p associated with this effect will not be considered. Equations (1) to (5) remain valid for infinitesimal changes $d\sigma_{ij}$ and de_{ij} and for current crack densities ρ_i . The elastic constants given by equations (4) now have the meaning of the tangent (current) elastic parameters. The dependence of crack densities, and, therefore, of elastic parameters on stresses leads to a nonlinear theory of elasticity.

Physical nonlinearity, i.e., the nonlinearity of stress-strain relations, will be considered. If the quantities p, ρ_i , σ_{ij} and e_{ij} depend on co-ordinates x_i , the stress-strain relations and the elastic parameters in (4) take on a local character.

For the assumed distribution of cracks (Fig.2), only the influence of compressive stress components σ_{11} , σ_{22} and σ_{33} on the three types of cracks characterised by densities ρ_1 , ρ_2 and ρ_3 , respectively, will be taken into account. Cracks of different radii r and openings 2b and of different aspect ratios b/r appear in the sprayed materials. With increasing pressure (for type 1 cracks with increasing value of negative stress component σ_{11}), the cracks with increasing aspect ratios b/r will gradually close. The dependence of crack densities on compressive stresses (e.g. ρ_1 on σ_{11}) should be based on distributions of the aspect ratios of these cracks. However, such distributions have not yet been determined from experiments.
In the recent paper [19], a linear dependence of the crack densities on the compressive stresses is assumed for simplicity,

$$\rho_i = \rho_{0i} (1 + \sigma_{ii}/k_i) , \quad i = 1, 2, 3, \quad -k_i \le \sigma_{ii} \le 0 . \qquad (7)$$

The crack densities without external stresses are denoted as ρ_{0i}, and $k_i>0$ are the limit values of closing pressures at which nearly all type 1, 2, 3 cracks are closed. Cracks with the aspect ratios b/r from 10^{-4} to 10^{-2} are expected in sprayed materials (cracks with higher aspect ratios contribute to porosity p), so that the limit closing pressures k_i of the order of 1GPa can be expected. The constants ρ_{0i} , k_i and p can be considered as new material constants of sprayed materials, which are, however, sensitive to the parameters of the spraying technology used.

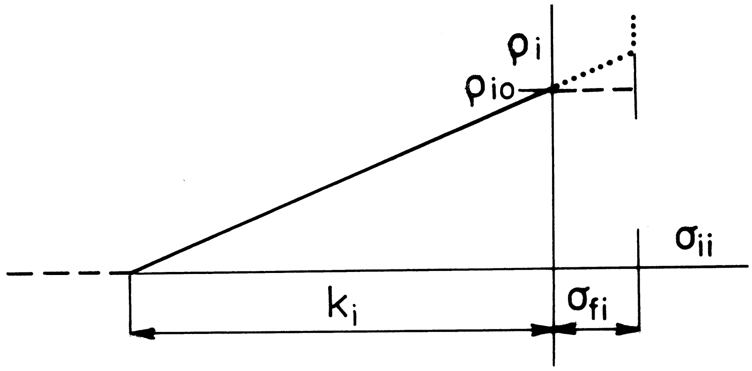

Fig.5. Proposed dependence of scalar crack densities ρ_i (i=1,2,3) on normal stress components σ_{ii} .

The dependence of ρ_i on σ_{ii} in eq.(7) and Fig.5 is proposed only for compressive stresses in the interval $-k_i \le \sigma_{ii} \le 0$. For higher values of compressive stresses, $\sigma_{ii}<-k_i$, all cracks are closed and $\rho_i=0$, as shown by the dashed line on the left side (only the effect of porosity remains).
For small tensile stresses, $0<\sigma_{ii}<\sigma_{fi}$, where σ_{fi} is the fracture stress (for plasma sprayed ceramics between 20 and 100 MPa), the crack densities could be only very roughly assumed constant, $\rho_i=\rho_{0i}$, as shown in Fig.5 by the dashed line on the right-hand side.
Young's tangent moduli E_i in eq.(4) depend, according to eq.(7), on compressive stresses σ_{ii} .
A physical model of the dependence of shear moduli G_{ij} on the crack densities must be specified. Two possibilities can be distinguished:

a. Free gliding along the crack surfaces under shear stress is allowed even for closed cracks. Shear moduli G_{ij} will then depend on the initial crack densities ρ_{0i} and, therefore, not on stresses σ_{ii} .
b. Restricted gliding by shear stresses along the surfaces of closed cracks may take place depending on the coefficient of friction and on the normal compressive stress component, as discussed in [14]. A complex inelastic behaviour then follows.

In paper [19], a reversible elastic theory according to case a. is proposed, i.e., free gliding along the surfaces of closed cracks is allowed, and the shear moduli G_{ij} are functions of the original crack densities ρ_{0i} but not of stresses σ_{ii} .
The tangent elastic parameters of the nonlinear material are now given by equations (4) with the proper choice of crack densities. Young's moduli E_i depend on normal stress components through the current crack densities ρ_i from eq.(7) in the following way: $E_1(\sigma_{11})$, $E_2(\sigma_{22})$, $E_3(\sigma_{33})$. On the other hand, the combinations of the elastic constants ν_{ij}/E_i , which characterise the lateral deformations, and the shear moduli G_{ij} do not depend on stresses. The tangent elastic parameters can be written in the form

$$
\begin{aligned}
1/E_i &= (1/E_0) \{ 1 + C_0 + A_{0i} + A_{0i}\, \sigma_{ii}/k_i \} , \quad i = 1, 2, 3, \quad -k_i \le \sigma_{ii} \le 0, \\
\nu_{ij}/E_i &= (1/E_0)\{ \nu_0 + C_1 \} , \quad i \neq j, \\
1/G_{ij} &= [2(1 + \nu_0)/E_0] \{ 1 + C_2 + A_{1i} + A_{1j} \}, \quad i \neq j
\end{aligned}
\tag{8}
$$

where the constants

$$
\begin{aligned}
&C_0 = [p/(1-p)]\, c_0 , \quad C_1 = [p/(1-p)]\, c_1 , \quad C_2 = [p/(1-p)]\, c_2 , \\
&A_{0i} = [1/(1-p)]\, a_0\, \rho_{0i} , \quad A_{1i} = [1/(1-p)]\, a_1\, \rho_{0i} , \quad i = 1, 2, 3.
\end{aligned}
\tag{9}
$$

All the constants in eq.(9) are positive, and they may be zero only in the trivial cases p=0 or ρ_{0i} =0.
Nonlinear stress-strain relations can now be obtained by elementary integration of relations (1) with (8) from zero to the final values of deformations e_{ij} and stresses σ_{ij} , with the result

$$
\begin{aligned}
e_{ii} &= (1/E_0) \{(1 + C_0 + A_{0i})\, \sigma_{ii} + (1/2)\, A_{0i}\, (1/k_i)\, \sigma_{ii}^2 - (\nu_0 + C_1)\, (\sigma_{jj} + \sigma_{kk})\} , \\
e_{ij} &= [(1+\nu_0)/E_0]\, \{1 + C_2 + A_{1i} + A_{1j}\}\, \sigma_{ij} , \quad i \neq j \neq k .
\end{aligned}
\tag{10}
$$

These relations are valid in the range of normal stress components $-k_i \le \sigma_{ii} \le 0$ .The material is anisotropic, of orthotropic symmetry. Its nonlinearity is manifested by occurrence of the second-order terms of stress components σ_{ii}^2 in expressions for e_{ii} . The integration is path independent and the conditions for the existence of the complementary elastic energy density are fulfilled.
The stress-strain relations (10) remain valid even for non-homogeneous deformation, with stresses σ_{ij} and strains e_{ij} dependent on co-ordinates x_i . They must comply with the linear equations of equilibrium and compatibility of the linear theory of elasticity, which form, together with nonlinear stress-strain relations (10), a system of nonlinear equations. A solution of such a system is not unique, although the solution with unique physical meaning can be found within the considered range of normal stresses in particular cases. Two simple examples will be discussed, uniaxial compression and pure bending.

Uniaxial compression
The stress-strain relations (10) will simplify for uniaxial compression in the x_1 direction, i.e., for $\sigma_{11}=\sigma$ and other $\sigma_{ij}=0$, to the form

$$
e = e_{11} = (1/E_0)\{(1 + C_0 + A_{01})\, \sigma + (1/2)\, A_{01}\, (1/k_1)\, \sigma^2\}, \quad -k_1 \le \sigma \le 0, \tag{11}
$$

$$e_{22} = e_{33} = -(1/E_0)(\nu_0 + C_1)\,\sigma, \quad e_{23} = e_{13} = e_{12} = 0.$$

Dimensionless stress σ/E_{10} will be introduced, where E_{10} is the value of tangent Young's modulus E_1 in eq.(8) for $\sigma_{11}\rightarrow 0$,

$$E_{10} = E_0 / [1 + C_0(p) + A_{01}(p, \rho_{01})] \,. \tag{12}$$

Equation (11) can then be written in the form

$$e = (\sigma/E_{10}) + C\,(\sigma/E_{10})^2 \tag{13}$$

where the constant

$$C = (1/2)\,A_{01}\,(E_{10}/E_0)\,(E_{10}/k_1). \tag{14}$$

The dependence of the tangent modulus on stress follows from eq.(8) or directly from (13) as $E_{tan} = 1/(de/d\sigma)$,

$$E_{tan} = E_{10} / [1 + 2\,C\,(\sigma/E_{10})], \tag{15}$$

while Young's secant modulus, $E_{sec} = 1/(e/\sigma)$,

$$E_{sec} = E_{10} / [1 + C\,(\sigma/E_{10})]. \tag{16}$$

To show some numerical results, a model plasma sprayed ceramic material will be introduced using the values ν_0=0.25, p=0.1 and ρ_{01}=0.5 so that from eq.(9) C_0=0.222, A_{01}=2.778 and from eq.(12) E_{10}=0.25 E_0 . The values of k_1 have not yet been measured. For expected values of ratios k_1/E_{10} between 1/60 and 1/120 the value of constant C from eq.(14) ranges between 20 and 40. The value C=30 will be chosen for the model material, corresponding to ratio k_1/E_{10}=1/86.4=0.0116. For example, for the model value E_0=250 GPa (estimated for γ-Al_2O_3) it is E_{10}=62.5 GPa and k_1=0.72 GPa.
The dependence $\sigma(e)$ for C=30 is shown in Fig.6 by the full curve in the region of compressive stresses $-k_1\leq\sigma\leq 0$, the proposed linear extension to higher compressive stresses and to small tensile stresses is plotted by the dashed lines. The limit elastic contraction e_L=-0.75 % corresponds to the limit compressive stress σ_L=-k_1 .
The stress dependences of corresponding tangent and secant Young's moduli in equations (15) and (16) are shown for C=30 in Fig.7. For the limit stress σ_L=-k_1 , the tangent modulus reaches the maximum value E_{tan}=3.27 E_{10}=0.818 E_0 due to remaining porosity p. For the same limit stress, the secant modulus reaches only the value E_{sec}=1.53 E_{10}=0.38 E_0 .
The difference Δ between the nonlinear solution and the linear solution $\sigma=E_{10}$ e , plotted by the dashed and dotted line, is also shown in Fig.6. With increasing elastic contraction, the nonlinear correction ranges from a few percent to tens of percent. This effect is less pronounced than the substantial increase of the tangent modulus.
A comment should be added on the uniqueness of the solution for the considered nonlinear material behaviour. For stress σ given in the interval $-k_1\leq\sigma\leq 0$, elastic strain e is obtained uniquely from eq.(13). However, if strain e is given, the corresponding stress must be calculated from quadratic algebraic equation (13) as $(\sigma/E_{10}) = [1/(2C)]\{-1\pm(1+4Ce)^{1/2}\}$. Only the solution with the + sign in front of the square root term has the physical meaning and is denoted in Fig.6 by the full line. The second solution with the - sign has no physical meaning,

nevertheless, it is shown in Fig.6 by the dotted line. The point with $E_{tan} = \infty$ on the non-physical curve corresponds to "forbidden stress" (σ/E_{10})=-1/(2C) and to "forbidden strain" e= -1/(4C), i.e., for C=30, to (σ/E_{10}) = -0.01666 and e= -0.8333 % .

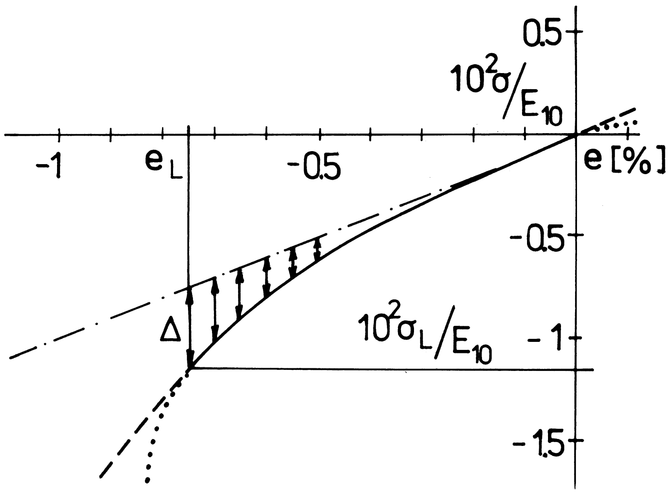

Fig.6. Stress-strain relation (13) for C=30.

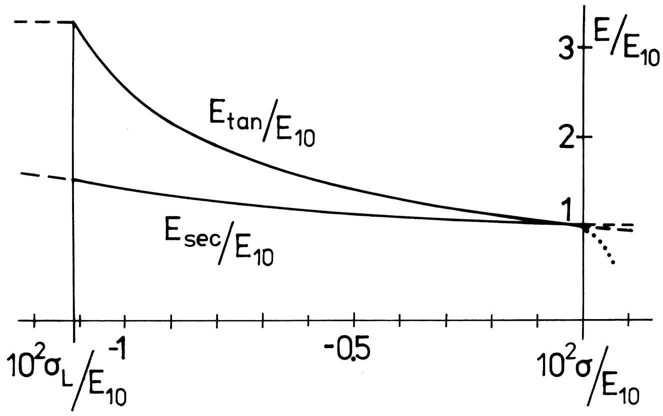

Fig.7. Stress dependences (15) and (16) of tangent and secant Young's moduli for C=30.

Bending

The bending of beams with coatings by external or residual stresses has been studied analytically in a number of papers within the linear theory of elasticity (see e.g. [20]). The results are used for determining the elastic constants of coatings or the residual stresses in coatings from analysis of the bending experiments. Consideration of the effect of compressive stresses on Young's moduli can improve these results. The solution of the nonlinear problem is more complex (F. Kroupa and J. Plesek, to be published). With increasing compressive stresses in the coating, the difference between the nonlinear and linear solution increases to tens of percent.

Experiments

The effect of compressive stresses on Young's moduli of plasma sprayed ceramics has already been proved, using two experimental methods.

The velocity of ultrasonic waves under hydrostatic pressure between 0 and 400 MPa in different directions in a sphere made of plasma sprayed alumina has recently been measured (T. Lokajíček and co-workers, to be published). The tangent Young's modulus evaluated from

these measurements increased from the original value $E_{10}\cong40$ GPa to $E_{tan}\cong120$ GPa. The saturation value (corresponding to the limit stress value σ_L) has not yet been reached.
An evaluation of the bending experiment of a zircon ($ZrSiO_4$) coating on a titanium substrate [21] showed, even at small compressive stresses up to σ=-24 MPa, an increase of Young's modulus of the coating from the original value $E_{10}\cong14$ GPa to $E_{tan}\cong24$ GPa. However, this experiment corresponds to uniaxial compressive stress and the elastic deformation was accompanied by inelastic deformation, similarly as in rocks [14].

TENSILE DEFORMATION AND SURFACE EFFECT

Tensile deformation
A few experiments have already shown that the strong nonlinear behaviour of sprayed materials appears also during tensile deformation, as shown schematically in Fig.6 by the dotted line on the right-hand side. This effect is obviously due to the increase of microcrack densities under tensile stresses. Some parts of interfaces between the splats and also some intrasplat cracks may be in mechanical contact, however, without bonding. These contact places do not act as microcracks under compression but they will elastically open under tensile stresses. Moreover, some local bonds may be so weak that they can be broken even at small tensile stresses and some microcracks can grow or new microcracks can be formed. Therefore, the crack densities will grow with increasing tensile stresses as shown in Fig.5 by the dotted line. This effect is not purely elastic, nevertheless, it is usually described as the decrease of Young's moduli with increasing tensile deformation, as shown schematically by the dotted line in Fig.7.

This effect is difficult to observe in free-standing parts where it can take place only at a small tensile deformation before fracture. On the other hand, it can be observed more easily in coatings where the integrity of the sprayed material is retained up to tensile deformations 0.1% or even 0.2% by constraint due to the metal substrate.
A nonlinear stress-strain curve in tension was measured for strains between 0 and 0.04% in plasma sprayed alumina coatings in the direction perpendicular to the spraying plane [22]. A decrease of Young's modulus from $E_{30}\cong30$ GPa to $E_3\cong15$ GPa was detected.

Surface effect
Stresses in the surface region of crystalline materials can be measured by X-ray diffraction, with the penetration depth for different wave lengths and different materials between 5 and 50 μm. The corresponding surface region in sprayed materials consists of few layers of splats only. Using X-ray diffraction, external stresses in the surface region of plasma sprayed coatings on the tensile side of metal substrates deformed in bending were measured in [23,24]. Surprisingly, the measured stresses were much lower than those which would correspond to Young's modulus E_{10} of the interior of the coating, which could be called the "volume effective" Young's modulus. To characterise the surface region, the "surface effective" Young's modulus $E_{1S}<E_{10}$ was introduced in [23,24]. For a plasma sprayed steel coating (with $E_0\cong200$ GPa) the values $E_{10}\cong90$ GPa and $E_{1S}\cong50$ GPa were measured in [23]. However, this surface effect is much stronger in ceramic coatings. For Cr_2O_3 coating (with $E_0\cong400$ GPa), the volume effective modulus $E_{10}\cong80$ GPa was measured in [24]. Surprisingly, the surface stresses measured be X-ray diffraction during increasing bending remained close to zero, within the measuring errors. Therefore, it was not possible to determine the surface effective value E_{1S} , thus approximately $E_{1S}\cong0$.

The surface effect can be explained by the behaviour of surface splats and splats close to the surface. New splats, formed by rapid solidification of impacted molten droplets and rapid cooling to the relatively low (deposition) temperature, are only weakly bonded along one interface with the previously deposited splats. The bonding of splats inside the coating improves by the following impact of new hot droplets and, moreover, the “inside” splats are bonded at both sides. Therefore, the surface and near surface splats are less bonded and the transmission of forces on the surface splats by shear stresses along the interfaces is weak and interface sliding may take place. Moreover, the intrasplat cracks in the surface splats open more easily, with no constraint at the free surface and a weak constraint at the interface. As a result, the tensile deformation of the surface region proceeds more easily, by combination of interface sliding and microcrack opening and this effect can be described by small surface effective Young’s modulus E_{1S}.
It is a macroscopic analogy to the surface properties of crystals. In the surface region consisting of two or three atomic layers, a relaxation leading to an increase of interatomic distances or to the formation of a special surface crystal structure takes place. The surface effective Young’s modulus is known to be different from the bulk value.

COMMENTS ON DELAMINATION AND FRACTURE OF COATINGS

Coatings delamination
The interface between the ceramic or metallic coating and the metal substrate is complex. The impacted molten droplets fill in the irregularities of the roughened substrate surface and the mechanical bonding seems to be an important contribution to the coating adhesion. The time of spreading of the droplet (of the order of μs) and of solidification and cooling of the splat to the substrate temperature (of the order of tens up to hundreds μs) is very short and only imperfect local bonds can develop by diffusion or chemical reactions. The areas of contact (called welding points or active zones) correspond only to 20% up to 30% of the total splat area [1].
The tensile bond strength σ_B , i.e., the tensile stress in direction perpendicular to the interface necessary for the coating delamination, is measured using different experimental configurations [25] , with smaller values for ceramic coatings ($\sigma_B \cong 10$ up to 50 MPa) than for metal coatings ($\sigma_B \cong 50$ up to 100 MPa). However, the measured value of σ_B depends on the chosen configuration and on the specimen dimensions.
In recent years, fracture mechanics of interfaces between different materials was developed [26]. The measured values of interface fracture toughness are very low for ceramic coatings, of the order of $K_{IC} \cong 1$ MPa $m^{1/2}$, and somewhat larger for metal coatings, especially if detonation spraying or vacuum plasma spraying is used.

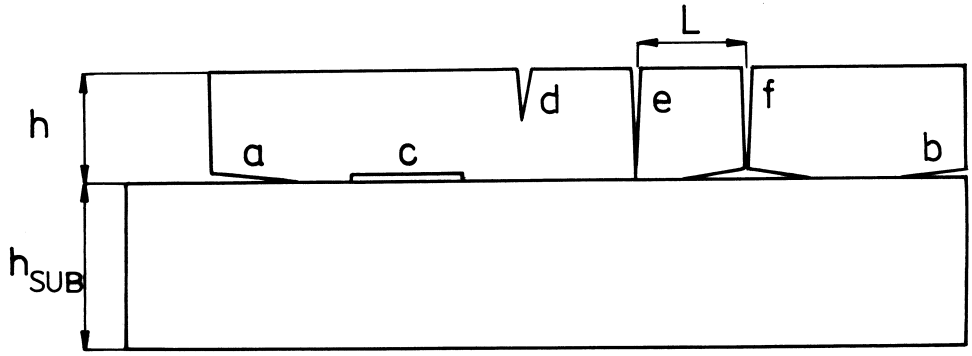

Fig.8. Delamination (a, b, c) and fracture (d, e, f) of a coating.

Delamination usually starts at the coating edges (positions a, b in Fig. 8) and only rarely inside the interface (position c). Delamination by buckling above a larger internal initial flaw c may be provided by high compressive residual stresses. High concentrations of external and also of residual stresses appear at the coating edges. The residual stresses are transferred to the coating via the concentrated shear stresses at the interface close to the edge, and these stress concentrations decrease the coating adhesion and may even lead to a spontaneous coating delamination [27]. Residual stresses usually grow with the coating thickness and, therefore, thicker coatings have poor adhesion. This effect can be used for preparation of free-standing ceramic parts from thick coatings. Using a higher substrate temperature, high secondary residual stresses form during cooling to the ambient temperature and, due to high stress concentrations at the edges, spontaneous delamination proceeds.

Fracture of free-standing parts

Plasma sprayed free-standing ceramic parts are anisotropic and have generally smaller strength and smaller fracture toughness than well sintered ceramics. The bending strength between 15 and 30 MPa is reported in [4] for different plasma sprayed ceramic materials. It can be improved by post-sintering or by different methods of impregnation. On the other hand, the thermal shock resistance of plasma sprayed ceramics is better because of lower elastic moduli and higher fracture strain due to the presence of microcracks.

A different technology called spray forming [28] is used for manufacture of free-standing metal parts. It is based on atomisation of a liquid metal stream into droplets which are propelled to the substrate. Because of the dense droplet stream and small dimensions of droplets, a fine scale microstructure with equiaxial grains, small porosity and without microcracks is formed. Alloys with high strength and fracture toughness and in a near net shape form can be manufactured by spray forming.

Fracture of coatings

Macrocracks perpendicular to the interface develop in coatings under higher tensile stresses, during tensile deformation or bending of the substrate with a coating on the tension face (Fig.8, d, e, f). The critical situation corresponds to penetration of microcracks from the near-surface splats to the interior splats and formation of a macrocrack by interconnection of the microcracks. The growth of the macrocrack is controlled by deformation of the substrate surface and starts in ceramic coatings at relative elongations between 0.1 and 0.2%. Usually, a steady state crack growth from a surface flaw in the directions along the surface and to the interface takes place (Fig.8, d). After reaching the interface, opening of the crack continues, sometimes connected with local plastic deformation of the substrate. In dependence on the substrate properties, the crack may even penetrate into the substrate. New macrocracks are formed with increasing substrate deformation and the coating separates into blocks. The loading of the blocks is induced by shear stresses along the interface. The density of cracks becomes saturated when the forces due to the shear stresses can no more exert sufficiently large tensile stresses necessary for formation of a new macrocrack in the middle of the block. The minimum distance L between the cracks (Fig.8) can be estimated from the condition $L/h \cong 2\,\sigma_F / \tau_F$ where σ_F is the tensile strength of the coating and τ_F is the shear strength of the interface [29, 30]. The cracks perpendicular to the interface then induce interface cracks (Fig. 8, f) and delamination of the blocks may proceed during increasing substrate elongation. The measured values of fracture toughness (for cracks growing in the direction perpendicular to the interface) are very low for ceramic coatings, $K_{IC} \cong 1$ MPa $m^{1/2}$, and somewhat larger for metal coatings, in dependence on the spraying technique used. However, in air plasma-

sprayed steel coatings, the splats are covered by oxides (the amount of oxides is about 10%) and $K_{IC} < 1$ MPa $m^{1/2}$ [31].
A large number of papers have already been published on failure of coatings under conditions corresponding to real-life situations, e.g., wear, cyclic deformation, high-temperature deformation, thermal shocks.

DISCUSSION

Mechanical properties of thermally sprayed materials, especially of ceramics, are substantially influenced by their specific mesoscopic defect structure—the high density of intersplat and intrasplat microcracks of dimensions between few μm to tens of μm. Even in the areas of good contact between the splats (outside the intrasplat microcracks) the bonding seems to be weaker than in well sintered materials.
In the previous literature (see e.g. [1]), the mechanical properties of these materials were considered as linear elastic at small and medium stresses, followed by brittle fracture at higher stresses. It is pointed out in this paper that, due to the mesoscopic defect structure, the mechanical behaviour at small and medium stresses is considerably nonlinear, for the main part elastically nonlinear under compressive stresses and inelastic under tensile stresses.
The decrease of Young's moduli caused by microcracks can be considered as a positive effect. The coatings can follow the deformation of the substrates up to strains 0.1% to 0.2% without formation of macroscopic cracks and have a good resistance against thermal shocks. However, for some applications the open porosity of ceramic coatings is disadvantageous. Therefore, sprayed metal bond coats between the ceramic coating and the substrate are often used, to improve the corrosion resistance. Metal bond coats also improve adhesion of the ceramic coatings. Mechanical properties can also be improved by application of different graded and layered coatings.

The metal substrate remains at relatively low temperature during the spraying process so that its structure does not change. Therefore, the substrate after its final optimum thermal treatment can be used. The attempts to improve the defect structure of the ceramic coatings by different methods of thermal surface treatment were not very successful [1] because of formation of cracks in the coatings, high residual stresses and delamination, appearing frequently during final cooling. For some applications, different methods of impregnation are used to eliminate the open porosity.
The coatings in as sprayed conditions are used in most applications and a certain optimalization of their mechanical properties can be achieved by a proper choice of the spraying technology and parameters. Formation of compressive residual stresses in coatings is usually advantageous.

It should be pointed out that the theoretical analysis of the elastic properties of sprayed materials explains well, in principle, the small values of Young's moduli and their dependence on compressive stresses. However, a detailed comparison of the theory with microscopic parameters, i.e., with the microcrack densities and their dependence on stress, has not yet been possible because of a lack of quantitative microscopic experiments. The total surface area of all cracks and pores was already measured in zirconia and alumina by small angle neutron scattering [32] and was found to be extremely large, of the order of 10^6 m^2/m^3, i.e., 10^4 cm^2/cm^3 or $1 \mu m^2/\mu m^3$. Unfortunately, this method does not give the dimensions of microcracks necessary for determination of the scalar crack densities introduced by eq.(3), which is decisive for the values of Young's moduli (Fig. 3). Neither the openings of the microcracks and the distribution of the crack aspect ratios, controlling the closing of microcracks under stress, have been measured; only a rough approximation is used in Fig. 5. Some systematic microscopic measurements of the crack dimensions and distributions would be very useful.

In spite of the extensive mesoscopic defect structure—microcracks and imperfect bonds—the thermally sprayed coatings, not only metallic but also ceramic ones, are quite good. They successfully improve the function and life-time of metal substrates in various applications, e.g., their wear, erosion, corrosion , chemical and thermal resistance.

Acknowledgements
The research is supported by GACR grant No.106/01/0094.

REFERENCES

[1] Pawlowski L: The Science and Engineering of Thermal Spray Coatings. J. Wiley, NewYork,1995.
[2] Clyne T.W. and Gill S.C.: J. of Thermal Spray Technology 5, (1996) 401.
[3] Neufuss K., Chráska P., Kolman B., Sampath S. and Trávníček Z.: J. of Thermal Spray Technology 6, (1997) 434.
[4] Lutz E.H.: Powder Metallurgy 25, (1993) 131.
[5] Li C-J., Ohmori A. and McPherson R.: In: Proceedings of AUSTCERAM 92, M.J. Bannister (Ed.). CSIRO, Melbourne,1992, pp. 816-821.
[6] Kroupa F.: Kovové materiály 33, (1995) 418.
[7] Kroupa F. and Kachanov M.: In: Proceedings of 19th Internat. Symp. on Materials Science, J.V. Carstensen et al. (Eds). Riso Nat. Lab., Roskilde, 1998, pp.325-330.
[8] Leigh L. and Berndt C.C.: Acta mater. 47, (1999) 1575.
[9] Sevostianov I. and Kachanov M.: Acta mater. 48, (2000) 1361.
[10] Hearmon R.F.S.: An Introduction to Applied Anisotropic Elasticity. Clarendon Press, Oxford, 1961.
[11] Kachanov M: Appl. Mech. Rev. 45, (1992), 304.
[12] Kachanov M., Tsukrov I. and Shafiro B.:Appl. Mech. Rev. 47, (1994), S 151.
[13] Walsh J.B.: J. of Geophysical Research 70, (1965), 381.
[14] Walsh J.B.: J. of Geophysical Research 70, (1965), 399.
[15] Brace W.F.: J. of Geophysical Research 70, (1965), 391.
[16] Pros Z., Lokajíček T. and Klíma K.: Pure and Applied Geophysics 151, (1998), 619.
[17] Pros Z., Lokajíček T., Přikryl R., Špičák A., Vajdová V. and Klíma K.: Pure and Applied Geophysics 151, (1998), 631.
[18] Kroupa F. and Dubsky J.: Scripta mater. 40, (1999), 1249.
[19] Kroupa F. and Plesek J.: Materials Sci. and Eng. A, in press.
[20] Kroupa F.: J. of Thermal Spray Technology 6, (1997), 309.
[21] Harok V. and Neufuss K.: J. of Thermal Spray Technology 10, (2001), 126.
[22] McPherson R.: Ceramics-Silikáty 35, (1991), 273.
[23] Dubsky J., Kolman B., Ctibor P., Kroupa F. and Ilavsky J.: In: Proceedings of 5th Internat. Symp. on Functionally Graded Materials 1998, W.A. Kaysser (Ed.). Trans. Tech Publications LTD, Switzerland, Materials Science Forum, Vols 308-311, 1999, pp. 232-237.
[24] Dubský J., Kolman B. and Vyšohlíd M.: In: Proceedings of United Thermal Spray Conference UTSC 99, E. Lugscheider and P.A Kammer (Eds). Verlag GmbH, Düsseldorf, 1999, pp. 659-663.
[25] Lin C.K. and Berndt C.C.: J. of Thermal Spray Technology 3,(1994), 75.

[26] Hutchinson J.W. and Suo Z.: Advances in Applied Mechanics 29, (1991), 63.
[27] Yu H.H., He M.Y.and Hutchinson J.W.: Acta mater. 49, (2001), 93.
[28] Grant P.S.: Progress in Materials Science 39, (1995), 497.
[29] Agrawal D.C. and Raj R.: Acta metall. 37, (1989), 1265.
[30] Thouless M.D.: J. of Am. Ceram. Soc. 73, (1990), 2144.
[31] Rabiei A., Mumm D.R., Hutchinson J.W., Schweinfest R., Rühle M. and Evans A.G.: Materials Sci. and Eng. A269, (1999), 152.
[32] Ilavsky J., Allen A.J., Long G.G., Krueger S., Berndt C.C. and Herman H.: J. of Am. Ceram. Soc. 80, (1997), 733.